

Effect of the preparation method on the catalytic performance of $\text{Ca}_3\text{Co}_4\text{O}_9$ for methane oxidation

Shaojie Feng · Wu Yang

Received: 15 December 2010 / Accepted: 28 December 2010 / Published online: 6 January 2011
© Springer Science+Business Media, LLC 2011

Abstract The layered structure oxide $\text{Ca}_3\text{Co}_4\text{O}_9$ particle was synthesized by two routes of citrate sol–gel method. The structure, morphology and surface property of $\text{Ca}_3\text{Co}_4\text{O}_9$ was characterized by XRD, SEM and XPS, respectively. The catalytic activity of $\text{Ca}_3\text{Co}_4\text{O}_9$ for methane combustion was tested in a fixed bed quartz tubular microreactor. The catalysis results reveal that the catalytic activity is sensitive to the texture of $\text{Ca}_3\text{Co}_4\text{O}_9$ by different route. TG measures confirm that the small particle size of $\text{Ca}_3\text{Co}_4\text{O}_9$ favors the oxygen transformation on the surface, which can be ascribed the random distribution of the crystal axes in irregular $\text{Ca}_3\text{Co}_4\text{O}_9$ particle.

Keywords $\text{Ca}_3\text{Co}_4\text{O}_9$ · Citrate sol–gel method · Methane · Catalytic combustion

1 Introduction

Recently, the misfit layered cobalt oxides $\text{Ca}_3\text{Co}_4\text{O}_9$ has received considerable attention due to its excellent thermoelectric property [1, 2]. Many efforts have been devoted to fabrication of textured $\text{Ca}_3\text{Co}_4\text{O}_9$ ceramics or single crystals of $\text{Ca}_3\text{Co}_4\text{O}_9$ and their thermoelectric properties [3–6]. On the other hand, it is reported that the $\text{Ca}_3\text{Co}_4\text{O}_9$ shows large range oxygen content variation depending on the temperature and partial pressure of oxygen [3, 7]. However, the property of oxygen nonstoichiometry in the

misfit-layered calcium cobalt oxides has not paid more attention to.

Catalytic oxidation of methane over metal oxides catalysts is an environmental friendly reaction because of a relatively low CO_2 emission for the same amount of energy production and lower NO_x formation in energy production. Some investigations indicate that the lattice oxygen is likely to be involved in the catalytic oxidation over cobalt oxide [8], and the reaction follows the Mars–Van Krevelen redox mechanism [9]. In this work, we prepared polycrystalline $\text{Ca}_3\text{Co}_4\text{O}_9$ material by two routes of citrate gel method and evaluated catalytic property of as-prepared $\text{Ca}_3\text{Co}_4\text{O}_9$ for methane oxidation reaction, with the aim to investigate the catalytic activity of oxygen vacancy and effect of particle texture on the catalytic property.

2 Experimental

2.1 Preparation

The $\text{Ca}_3\text{Co}_4\text{O}_9$ was synthesized by two routes of citrate gel method.

$\text{Ca}_3\text{Co}_4\text{O}_9$ -A: An aqueous solution containing calcium and cobalt nitrate (Ca/Co molar ratio = 0.75), and citric acid ($\text{citric acid}/(\text{Ca} + \text{Co}) = 1.3$) was gradually heated to 80 °C resulting in the formation of a gel. The gel was kept at this temperature for 4 h with stirring and dried at 120 °C for 12 h. The dried was burned using anhydrous ethanol as the igniter. The obtained ash was pulverized and then calcined at 900 °C for 10 h.

$\text{Ca}_3\text{Co}_4\text{O}_9$ -B: In this method, a dispersant of polyethylene glycol (PEG) 400 (2% volume ratio) was added in the mixture solution of metal ions and citric acid (similar to Process A). The solution was heated at 80 °C to obtain the

S. Feng (✉) · W. Yang
School of Materials Science and Chemical Engineering,
Anhui University of Architecture, 230022 Hefei, Anhui,
People's Republic of China
e-mail: fengshaojie@aiai.edu.cn

gel. The gel was dried at 120 °C for 12 h and then heat treated in the air at 500 °C for 2 h. Finally, the ash was calcined at 900 °C for 9 h.

2.2 Characterization

The crystalline structure of the catalysts was characterized by X-ray diffraction (XRD) using Ni-filtered Cu $K\alpha$ radiation ($\lambda = 1.5406\text{\AA}$) (Rigaku D/Max- γ A, Japan). The morphology of the particles was examined using field emission scanning electron microscopy (JEOL 6500F). X-ray photoelectron spectroscopy (XPS) measurements were performed with Mg $K\alpha$ (1,253.6 eV) as the exciting radiation (ESCALAB Mark II, VG). Thermogravimetric analyses (TGA) were performed for the as-air-synthesized sample in a nitrogen stream at a heating rate of 10 °C min⁻¹ (STA449C, Netzsch).

2.3 Catalysis test

Catalytic tests were carried out in a fixed bed reactor constituted of a quartz tube with an inner diameter of 4 mm at the atmospheric pressure. The feed consisted of a mixture of 2 mol% CH₄, 20 mol% O₂ and N₂ balance, with total gas hourly space velocity (GHSV) of 76,000 h⁻¹. The effluent composition was determined using on-line gas chromatography (Shimadzu, GC-14C) using a thermal conductivity detector (TCD) equipped with two columns, in which N₂, O₂ and CH₄ were separated by 5 Å molecular sieve column and CO₂, C₂H₄ and C₂H₆ by GDX-502 column.

3 Results and discussion

Figure 1 shows the X-ray diffraction (XRD) patterns of two as-prepared Ca₃Co₄O₉ samples. The XRD patterns show same polycrystalline misfit layered cobalt oxides Ca₃Co₄O₉ structure (JCPDS File Card No. 23-0110) mainly. There was no evident diffraction peak referring to Ca₃Co₂O₆, or CaO and CoO. However, a small amount of Ca₂Co₂O₅ phase (JCPDS File Card No. 37-0668) was found in two of samples. The Ca₂Co₂O₅ is reported to exhibit a considerably same misfit layered crystal structure with Ca₃Co₄O₉ possessing 25% Ca site vacancy [10]. Thus, the most diffraction peaks of the two phases are overlapped. The c-lattice parameter, computed using d-spacing values of (00l) reflections, was found to be 10.83 Å, which is in agreement with the reported value [1].

Figure 2 shows the SEM micrographs of the Ca₃Co₄O₉-A and Ca₃Co₄O₉-B particles. It is obvious that the dispersant and heat treatment condition has distinct effects on the crystal growth though are plate-like particles observed at

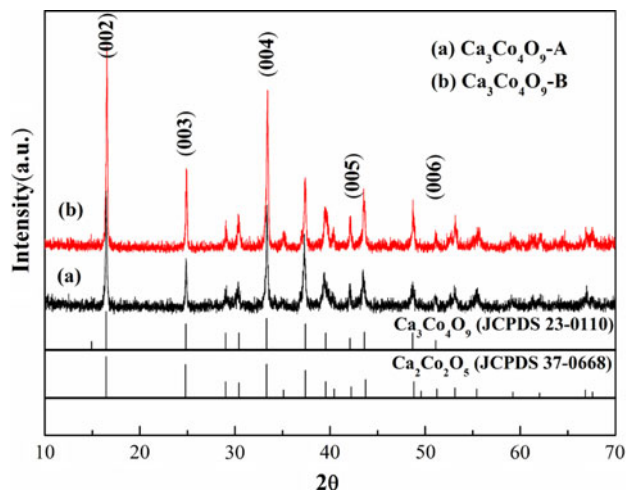


Fig. 1 XRD patterns of Ca₃Co₄O₉

higher magnification micrograph ((b) and (d)). Ca₃Co₄O₉-A sample is irregular in size distribution and shape of particles. In comparison, the Ca₃Co₄O₉-B sample is homogeneous and high textured.

Figure 3 presents CH₄ conversion plots obtained over two Ca₃Co₄O₉ samples. It can be seen that two samples exhibited a remarkable difference in methane oxidation reaction at the same condition. Ca₃Co₄O₉-A is more active than Ca₃Co₄O₉-B, the light-off temperature was about 500 °C, T₁₀ and T₉₀ were 575, 725 °C respectively. In contrast, the light-off temperature was about 700 °C in Ca₃Co₄O₉-B.

It is well accepted that gas-phase oxygen molecules are activated through an interaction with the surface of the catalyst for methane deep oxidation over metal oxides [11]. At first, the surface oxygen species on Ca₃Co₄O₉ was studied by XPS O1 s spectrum. As shown in Fig. 4, two samples reveal almost same surface oxygen property; a good curve fitting is obtained with three resolved O1s XPS peaks. The first peak with low binding energy (~529.1 eV) corresponded to CoO₂ layer on the surface. The second peak at binding energy (~531.3 eV) is usually ascribed to CaO layer species on the surface [12]. The minimal peak at binding energy about 533.4 eV may be assigned to adsorbed water molecules from humidity. Therefore, it can be concluded that the oxygen species on Ca₃Co₄O₉ surface don't cause the difference of catalytic oxidation of methane at this condition.

Secondly, we investigated the oxygen transformation on the surface of Ca₃Co₄O₉ by thermoanalysis measure of the as-synthesized Ca₃Co₄O₉ in a flowing nitrogen stream, as shown in Fig. 5. The overall weight loss observed in two samples can be divided into three processes from room temperature to 1,000 °C. The first weight loss before 500 °C could be assigned to desorption of the surface

Fig. 2 SEM micrographs of $\text{Ca}_3\text{Co}_4\text{O}_9$ particles.
a,b $\text{Ca}_3\text{Co}_4\text{O}_9$ -A;
c,d $\text{Ca}_3\text{Co}_4\text{O}_9$ -B

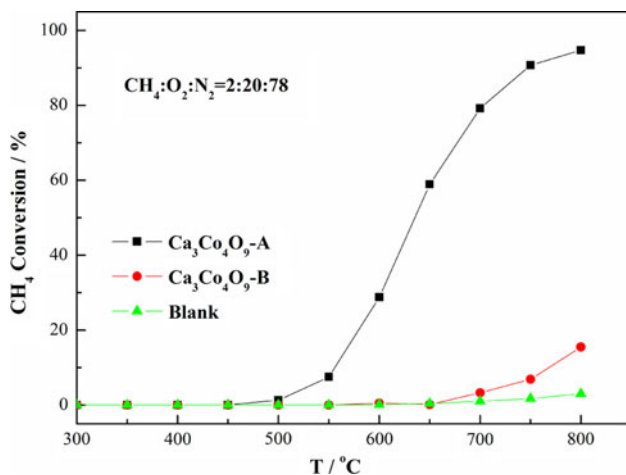
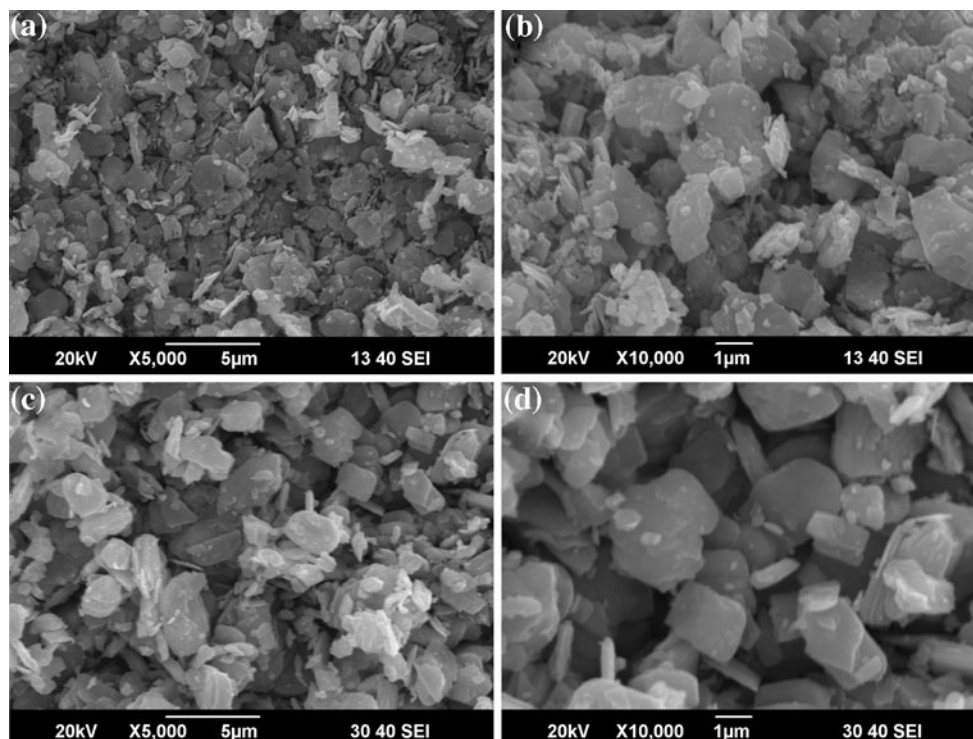


Fig. 3 CH_4 conversion plots over $\text{Ca}_3\text{Co}_4\text{O}_9$

adsorbed oxygen species, which is adsorbed in the structure defects (oxygen vacancies). It is notable that at about 510 °C there is a small but visible change in the slope of the TG curve. The same phenomenon has been observed by Y. Morita and is suggested as a possible phase transition point [13]. The second weight loss between 500 and 850 °C can be accounted for loss of surface lattice oxygen resulting in oxygen vacancy formation. The third weight loss possessing two successive weight losses between 850 and 1,000 °C is assigned to the decomposition of $\text{Ca}_3\text{Co}_4\text{O}_9$. Although the $\text{Ca}_3\text{Co}_4\text{O}_9$ phase transforms to

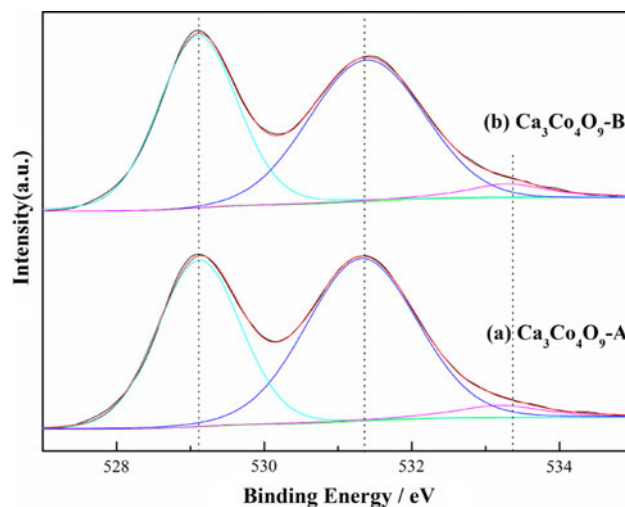


Fig. 4 XPS spectra of $\text{Ca}_3\text{Co}_4\text{O}_9$ for the O1 s regions

$\text{Ca}_3\text{Co}_2\text{O}_6$ phase at 950 °C in air atmosphere [14], it is predictable that the decomposition temperature of $\text{Ca}_3\text{Co}_4\text{O}_9$ will move towards lower temperature in nitrogen atmosphere. Therefore, $\text{Ca}_3\text{Co}_4\text{O}_9$ was likely to decompose to $\text{Ca}_3\text{Co}_2\text{O}_6$ at 850 °C firstly, and then, $\text{Ca}_3\text{Co}_2\text{O}_6$ decomposed to CaO and CoO finally.

However, two samples gave different dynamic behavior of oxygen desorption during N_2 annealing. The weight loss in $\text{Ca}_3\text{Co}_4\text{O}_9$ -A is bigger than that in $\text{Ca}_3\text{Co}_4\text{O}_9$ -B at the same condition suggesting that desorption of oxygen

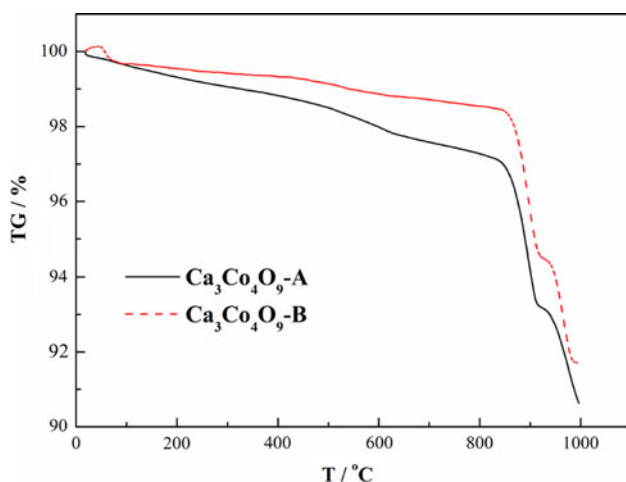
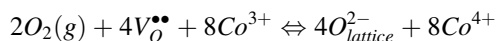


Fig. 5 TGA curves of the fresh $\text{Ca}_3\text{Co}_4\text{O}_9$ sample in flowing nitrogen

species in $\text{Ca}_3\text{Co}_4\text{O}_9$ -A is easy. $\text{Ca}_3\text{Co}_4\text{O}_9$ has a layered structure in which two different kinds of Co–O layers alternate in the direction of the *c*-axis. In one of the layers, Co atom is in an octahedral configuration and the octahedra are edge-shared (CoO_2 layers). In the other layers, Ca, Co and O form triple rock-salt ($\text{Ca}_2\text{CoO}_{3+\delta}$) layers [5]. M. Karppinen et al. [13, 15] investigated the oxygen nonstoichiometry of the $\text{Ca}_3\text{Co}_4\text{O}_9$ and supposed that all vacancies are in the CoO layer of the insulating Ca_2CoO_3 block. In this block, the CoO layer is sandwiched in between two CaO layers. As a result, the oxygen exchange between gas and crystal lattice in small particle of $\text{Ca}_3\text{Co}_4\text{O}_9$ -A is easier than that of $\text{Ca}_3\text{Co}_4\text{O}_9$ -B by the random distribution of the crystal axes, as given by



4 Conclusions

Two layered structure oxide $\text{Ca}_3\text{Co}_4\text{O}_9$ particles were successfully synthesized by different routes of citrate gel method. XRD and XPS confirmed there was no obvious

difference in structure and surface oxygen property for two samples. The catalytic tests revealed that two $\text{Ca}_3\text{Co}_4\text{O}_9$ particles exhibit distinct activity for combustion of methane. Based on the SEM results and TGA data, we suppose that small irregular $\text{Ca}_3\text{Co}_4\text{O}_9$ particle with random distribution of the crystal axes favors the oxygen transformation on the surface and catalytic activity.

Acknowledgments The authors acknowledge support from the Nature Science Foundation of the Department of Education of Anhui (KJ2009A023Z) and the Open Fund of Anhui Key Laboratory of Controllable Chemistry Reaction and Material Chemical Engineering.

References

1. Masset AC, Michel C, Maignan A, Hervieu M, Toulemonde O, Studer F, Raveau B (2000) *Phys Rev B* 62:166–175
2. Matsubara I, Funahashi R, Takeuchi T, Sodeoka S (2001) *J Appl Phys* 90:462–465
3. Masuda Y, Nagahama D, Itahara H, Tani T, Seo WS, Koumoto K (2003) *J Mater Chem* 13:1094–1099
4. Tani T, Itahara H, Xia CT, Sugiyama J (2003) *J Mater Chem* 13:1865–1867
5. Zhang Y, Zhang J, Lu Q (2007) *Ceram Int* 33:1305–1308
6. Bhattacharya S, Aswal DK, Singh A, Thinakaran C, Kulkarni N, Gupta SK, Yakhmi JV (2005) *J Cryst Growth* 277:246–251
7. Shimoyama J, Horii S, Otszchi K, Sano M, Kishio K (2003) *Jpn J Appl Phys* 42:L194–L197
8. Arnone S, Bagnasco G, Busca G, Lisi L, Russo G, Turco M (1998) *Stud Surf Sci Catal* 119:65–70
9. Bahlawane N (2006) *Appl Catal B* 67:168–176
10. Vidyasagar K, Gopalakrishnan J, Rao CNR (1984) *Inorg Chem* 23:1206–1210
11. Sokolovskii VD (1990) *Catal Rev* 32:1–49
12. Wakisaka Y, Hirata S, Mizokawa T, Suzuki Y, Miyazaki Y, Kajitani T (2008) *Phys Rev B* 78:235107
13. Morita Y, Poulsen J, Sakai K, Motohashi T, Fujii T, Terasaki I, Yamauchi H, Karppinen M (2004) *J Solid State Chem* 177:3149–3155
14. Zhang Y, Zhang J, Lu Q, Zhang Q (2006) *Mater Lett* 60:2443–2446
15. Karppinen M, Fjellvåg H, Konno T, Morita Y, Motohashi T, Yamauchi H (2004) *Chem Mater* 16:2790–2793